

Electronic Supplementary Information

Tunneling Effect in Vitamin E Recycling by Green Tea

Shin-ichi Nagaoka,* Akiko Nitta, Ai Suemitsu and Kazuo Mukai

*Department of Chemistry, Faculty of Science and Graduate School of Science and
Engineering, Ehime University, Matsuyama 790-8577, Japan*

*Corresponding author: Shin-ichi Nagaoka

e-mail: nagaoka@ehime-u.ac.jp

Phone: 81-89-927-9592

Fax: 81-89-927-9590

Table S1 k_r^H , k_r^D , k_s^H , k_s^D , $2k_d^H$ and $2k_d^D$ values for reactions (1)–(3) in EtOH/H₂O and EtOD/D₂O at 15–37 °C.

Fig. S1 Rise-and-decay curves of [α -Toc•] during reaction (2-H) and the subsequent reaction (3-H) in EtOH/H₂O at 15–37 °C, and the curves simulated according to eqns (9)–(16).

Fig. S2 Rise-and-decay curves of [α -Toc•] during reaction (2-D) and the subsequent reaction (3-D) in EtOD/D₂O at 15–37 °C, and the curves simulated according to those similar to eqns (9)–(16).

Fig. S3 Arrhenius plots of k_s^H and k_s^D values for reactions (2-H) and (2-D) in EtOH/H₂O and EtOD/D₂O, respectively.

Fig. S4 Decay curves of α -Toc• absorbance at 429 nm during reaction (3-D) and the competitive reaction (1-D) between α -Toc• and EGC-D in EtOD/D₂O at 25 °C.

Fig. S5 Decay curves of α -Toc• absorbance at 429 nm during reaction (3-H) and the competitive reaction (1-H) between α -Toc• and EC-H in EtOH/H₂O at 25 °C.

Fig. S6 Decay curves of α -Toc• absorbance at 429 nm during reaction (3-D) and the competitive reaction (1-D) between α -Toc• and EC-D in EtOD/D₂O at 25 °C.

Fig. S7 Decay curves of α -Toc• absorbance at 429 nm during reaction (3-H) and the competitive reaction (1-H) between α -Toc• and ECG-H in EtOH/H₂O at 25 °C.

Fig. S8 Decay curves of α -Toc• absorbance at 429 nm during reaction (3-H) and the competitive reaction (1-H) between α -Toc• and EGCG-H in EtOH/H₂O at 25 °C.

Fig. S9 Decay curves of α -Toc• absorbance at 429 nm during reaction (3-D) and the competitive reaction (1-D) between α -Toc• and EGCG-D in EtOD/D₂O at 25 °C.

Fig. S10 Decay curves of α -Toc• absorbance at 429 nm during reaction (3-H) and the competitive reaction (1-H) between α -Toc• and MR in EtOH/H₂O at 25 °C.

Fig. S11 Decay curves of α -Toc• absorbance at 429 nm during reaction (3-H) and the competitive reaction (1-H) between α -Toc• and MC in EtOH/H₂O at 25 °C.

Fig. S12 Decay curves of α -Toc• absorbance at 429 nm during reaction (3-H) and the competitive reaction (1-H) between α -Toc• and MG in EtOH/H₂O at 25 °C.

Fig. S13 Arrhenius plot of k_r^H values for reaction (1-H) between α -Toc• and EC-H in EtOH/H₂O.

Fig. S14 Arrhenius plot of k_r^H values for reaction (1-H) between α -Toc• and ECG-H in EtOH/H₂O.

Fig. S15 Arrhenius plot of k_r^H values for reaction (1-H) between α -Toc• and EGCG-H in EtOH/H₂O.

Fig. S16 Arrhenius plot of k_r^D values for reaction (1-D) between α -Toc• and EGCG-D in EtOD/D₂O.

Fig. S17 Arrhenius plot of k_r^H values for reaction (1-H) between α -Toc• and MC in EtOH/H₂O.

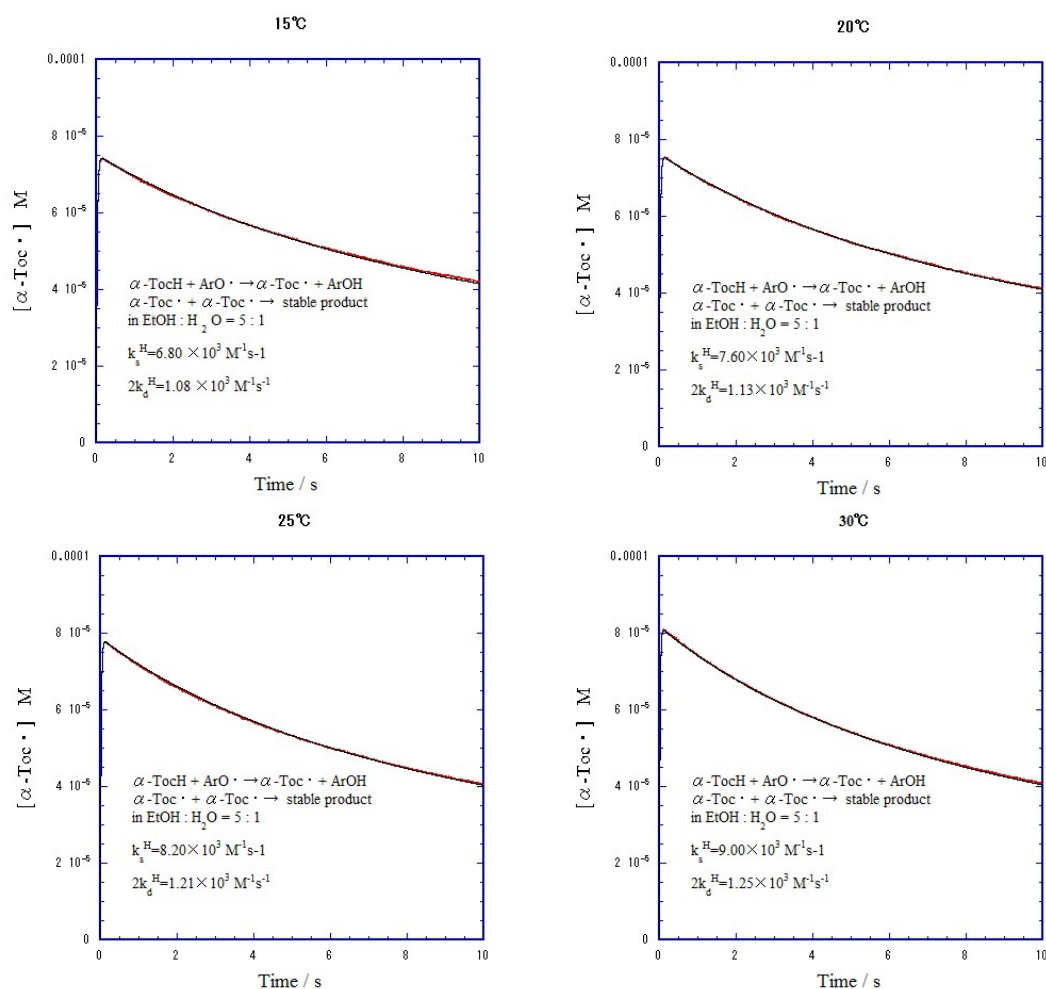
Fig. S18 Arrhenius plot of k_r^H values for reaction (1-H) between α -Toc• and MG in EtOH/H₂O.

Table S1 k_r^H , k_r^D , k_s^H , k_s^D , $2k_d^H$ and $2k_d^D$ values for reactions (1)–(3) in EtOH/H₂O and EtOD/D₂O at 15–37 °C

Molecule		Reaction rate constant / M ⁻¹ s ⁻¹				
		15	20	25	30	37 / °C
EC-H	k_r^H	7.90×10^2	9.63×10^2	1.20×10^3	1.46×10^3	1.78×10^3
EC-D	k_r^D	- ^a	- ^a	2.56×10^2	3.28×10^2	- ^a
ECG-H	k_r^H	2.38×10^3	2.84×10^3	3.43×10^3	4.18×10^3	5.22×10^3
ECG-D	k_r^D	- ^a	- ^a	- ^a	- ^a	- ^a
EGC-H	k_r^H	2.00×10^4	2.24×10^4	2.41×10^4	2.71×10^4	2.98×10^4
EGC-D	k_r^D	- ^a	2.23×10^3	2.49×10^3	3.00×10^3	3.74×10^3
EGCG-H	k_r^H	1.82×10^4	2.02×10^4	2.31×10^4	2.50×10^4	2.83×10^4
EGCG-D	k_r^D	- ^a	- ^a	4.49×10^3	5.30×10^3	6.89×10^3
MR	k_r^H	$< 10^2$	$< 10^2$	$< 10^2$	$< 10^2$	$< 10^2$
MC	k_r^H	3.30×10^3	3.96×10^3	4.48×10^3	5.38×10^3	6.32×10^3
MP	k_r^H	1.38×10^5	1.61×10^5	1.75×10^5	1.87×10^5	1.88×10^5
MG	k_r^H	1.47×10^3	1.78×10^3	2.11×10^3	2.46×10^3	3.06×10^3
α -TocH	k_s^H	6.80×10^3	7.50×10^3	8.20×10^3	9.00×10^3	1.00×10^4
α -TocD	k_s^D	2.70×10^2	3.20×10^2	4.00×10^2	4.55×10^2	5.45×10^2
α -Toc•	$2k_d^H$	1.08×10^3	1.13×10^3	1.21×10^3	1.25×10^3	1.40×10^3
α -Toc•	$2k_d^D$	8.80×10^2	8.90×10^2	9.50×10^2	1.01×10^3	1.15×10^3

^a Reliable data was not obtained.

Fig. S1 Rise-and-decay curves of $[\alpha\text{-Toc}\cdot]$ during reaction (2-H) and the subsequent reaction (3-H) in EtOH/H₂O at 15–37 °C (red curves), and the curves simulated according to eqns (9)–(16) (black curves). In the simulation, k_s^H and $2k_d^H$ are set to the values given in Table S1, and $[\text{ArO}\cdot]_0$ are set to 7.50×10^{-2} , 7.60×10^{-2} , 7.85×10^{-2} , 8.15×10^{-2} and 8.46×10^{-2} mM at 15, 20, 25, 30 and 37 °C, respectively. $[\alpha\text{-TocH}]_0 = 6.33$ mM and $\varepsilon = 3420$ M⁻¹cm⁻¹.



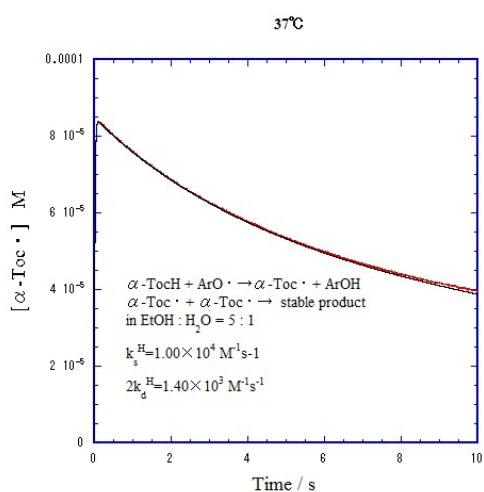
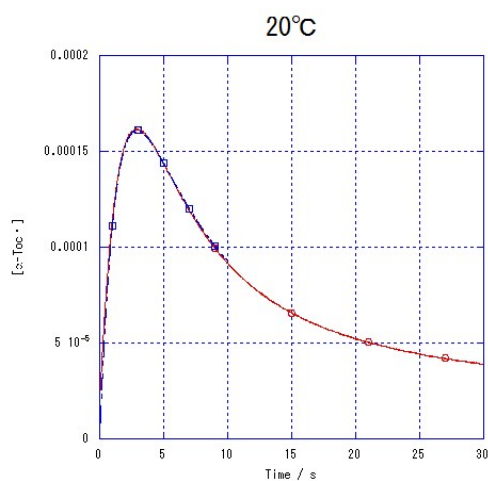
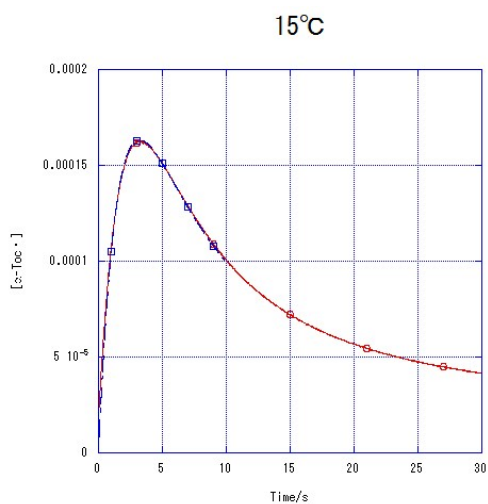


Fig. S2 Rise-and-decay curves of $[\alpha\text{-Toc}\cdot]$ during reaction (2-D) and the subsequent reaction (3-D) in EtOD/D₂O at 15–37 °C (red curves), and the curves simulated according to those similar to eqns (9)–(16) (blue curves). In the simulation, k_s^D and $2k_d^D$ are set to the values given in Table S1, and $[\text{ArO}\cdot]_0$ are set to 0.255, 0.240, 0.230, 0.218 and 0.215 mM at 15, 20, 25, 30 and 37 °C, respectively. $[\alpha\text{-TocD}]_0 = 2.12$ mM and $\varepsilon = 3420$ M⁻¹cm⁻¹.



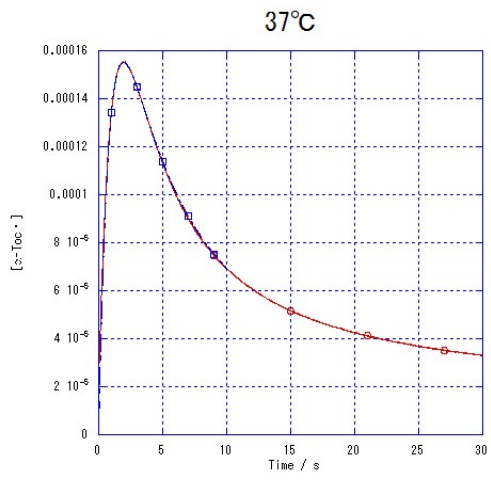
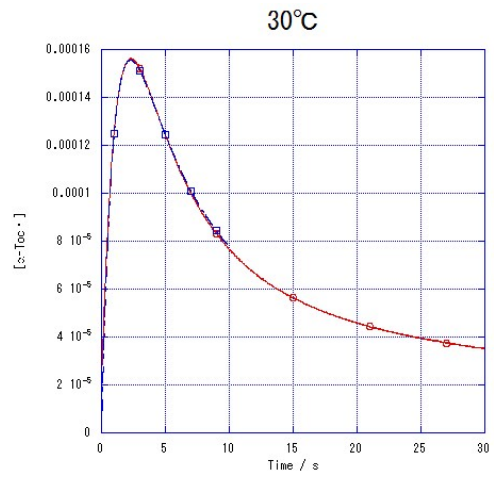
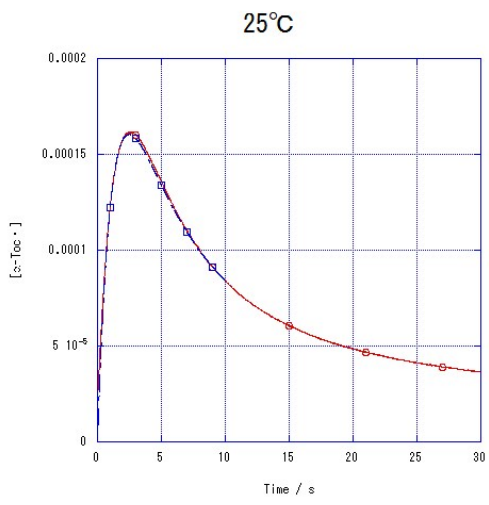


Fig. S3 Arrhenius plots of k_s^H and k_s^D values for reactions (2-H) and (2-D) in EtOH/H₂O and EtOD/D₂O (open and filled circles, respectively). The solid lines show the best-fitting lines by standard linear least-squares analyses.

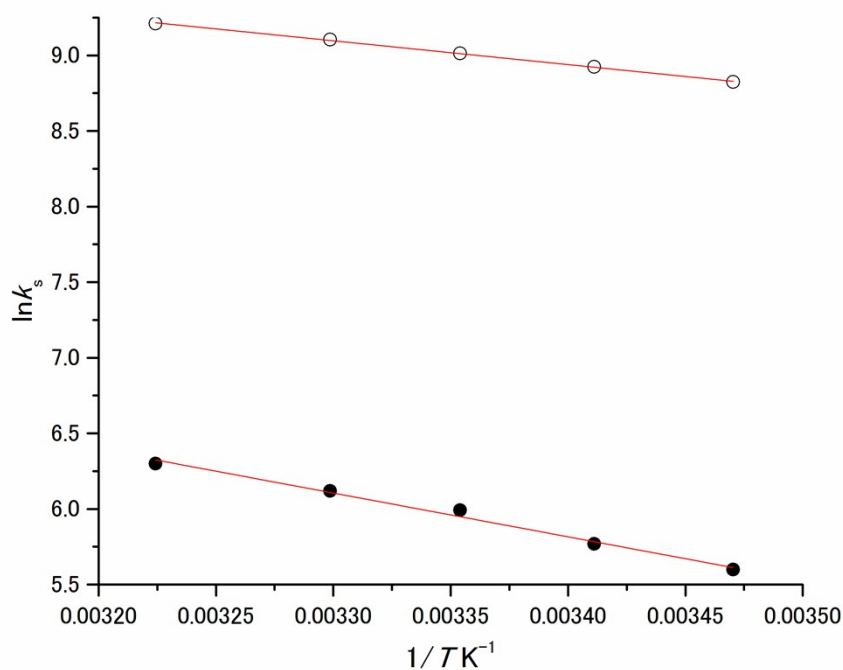


Fig. S4 Decay curves of α -Toc• absorbance at 429 nm during reaction (3-D) and the competitive reaction (1-D) between α -Toc• and EGC-D in EtOD/D₂O at 25 °C. The prepared [EGC-D] for the data shown with red, blue, green and black curves were 3.96×10^{-5} , 7.92×10^{-5} , 1.19×10^{-4} and 1.58×10^{-4} M, respectively.

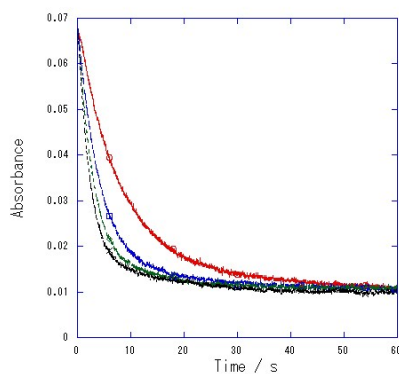


Fig. S5 Decay curves of α -Toc• absorbance at 429 nm during reaction (3-H) and the competitive reaction (1-H) between α -Toc• and EC-H in EtOH/H₂O at 25 °C. The prepared [EC-H] for the data shown with black, dark-grey, red and light-gray curves were 3.57×10^{-4} , 7.14×10^{-4} , 1.07×10^{-3} and 1.43×10^{-3} M, respectively.

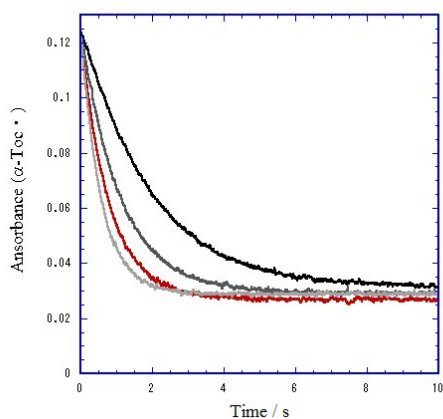


Fig. S6 Decay curves of α -Toc• absorbance at 429 nm during reaction (3-D) and the competitive reaction (1-D) between α -Toc• and EC-D in EtOD/D₂O at 25 °C. The prepared [EC-D] for the data shown with red, blue, green and black curves were 3.44×10^{-4} , 6.88×10^{-4} , 1.03×10^{-3} and 1.38×10^{-3} M, respectively.

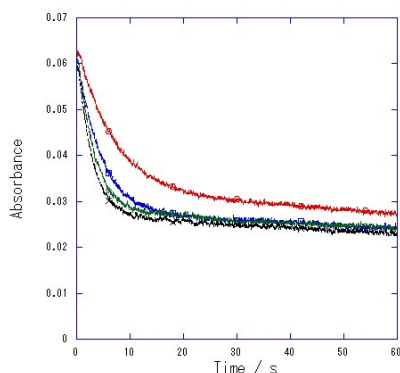


Fig. S7 Decay curves of α -Toc• absorbance at 429 nm during reaction (3-H) and the competitive reaction (1-H) between α -Toc• and ECG-H in EtOH/H₂O at 25 °C. The prepared [ECG-H] for the data shown with black, dark-grey, red and light-gray curves were 3.84×10^{-5} , 7.69×10^{-5} , 1.15×10^{-4} and 1.53×10^{-4} M, respectively.

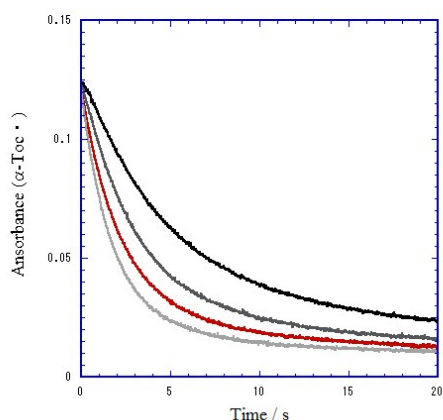


Fig. S8 Decay curves of α -Toc• absorbance at 429 nm during reaction (3-H) and the competitive reaction (1-H) between α -Toc• and EGCG-H in EtOH/H₂O at 25 °C. The prepared [EGCG-H] for the data shown with black, dark-grey, red and light-gray curves were 1.79×10^{-5} , 3.58×10^{-5} , 5.38×10^{-5} and 7.17×10^{-5} M, respectively.

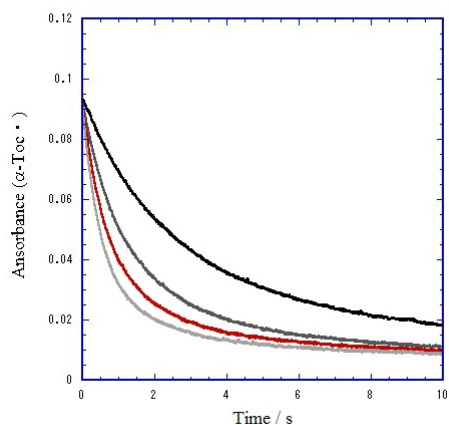


Fig. S9 Decay curves of α -Toc \cdot absorbance at 429 nm during reaction (3-D) and the competitive reaction (1-D) between α -Toc \cdot and EGCG-D in EtOD/D₂O at 25 °C. The prepared [EGCG-D] for the data shown with red, blue, green and black curves were 3.20×10^{-5} , 6.39×10^{-5} , 9.56×10^{-5} and 1.28×10^{-4} M, respectively.

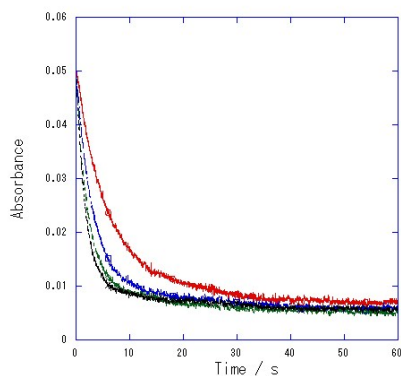


Fig. S10 Decay curves of α -Toc \cdot absorbance at 429 nm during reaction (3-H) and the competitive reaction (1-H) between α -Toc \cdot and MR in EtOH/H₂O at 25 °C. The prepared [MR] for the data shown with black, dark-grey, red and light-gray curves were 9.18×10^{-4} , 1.84×10^{-3} , 2.75×10^{-3} and 3.67×10^{-3} M, respectively.

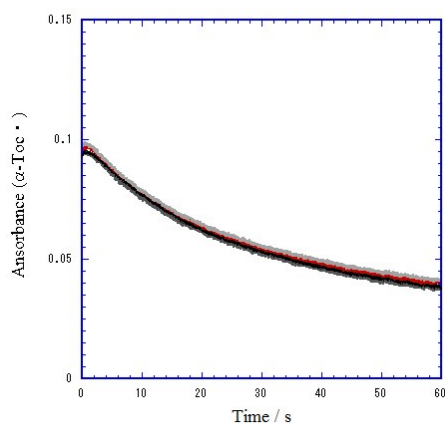


Fig. S11 Decay curves of α -Toc• absorbance at 429 nm during reaction (3-H) and the competitive reaction (1-H) between α -Toc• and MC in EtOH/H₂O at 25 °C. The prepared [MC] for the data shown with black, dark-grey, red and light-gray curves were 1.07×10^{-3} , 2.14×10^{-3} , 3.20×10^{-3} and 4.27×10^{-3} M, respectively.

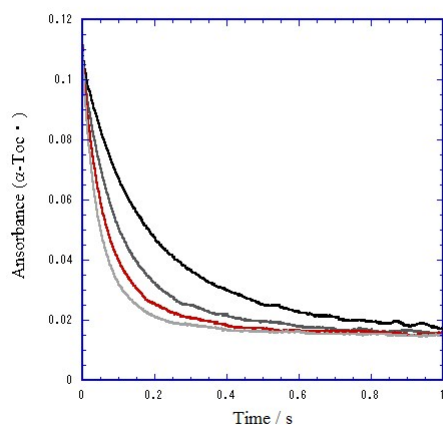


Fig. S12 Decay curves of α -Toc• absorbance at 429 nm during reaction (3-H) and the competitive reaction (1-H) with MG in EtOH/H₂O at 25 °C. The prepared [MG] for the data shown with black, dark-grey, red and light-gray curves were 6.44×10^{-4} , 1.29×10^{-3} , 1.93×10^{-3} and 2.58×10^{-3} M, respectively.

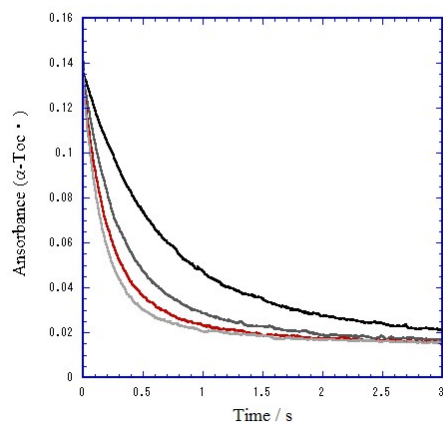


Fig. S13 Arrhenius plot of k_r^H values for reaction (1-H) between α -Toc• and EC-H in EtOH/H₂O. The solid line shows the best-fitting line by a standard linear least-squares analysis.

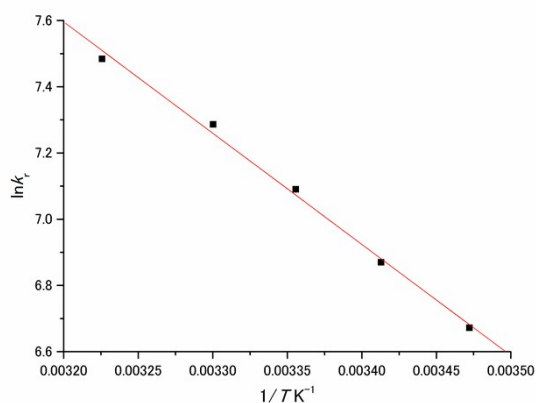


Fig. S14 Arrhenius plot of k_r^H values for reaction (1-H) between α -Toc• and ECG-H in EtOH/H₂O. The solid line shows the best-fitting line by a standard linear least-squares analysis.

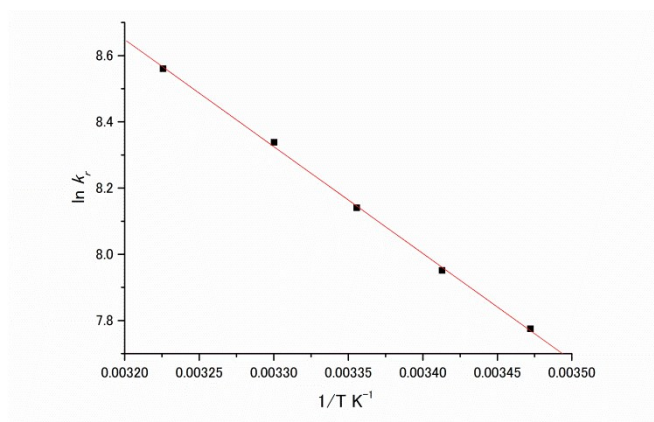


Fig. S15 Arrhenius plot of k_r^H values for reaction (1-H) between α -Toc• and EGCG-H in EtOH/H₂O. The solid line shows the best-fitting line by a standard linear least-squares analysis.

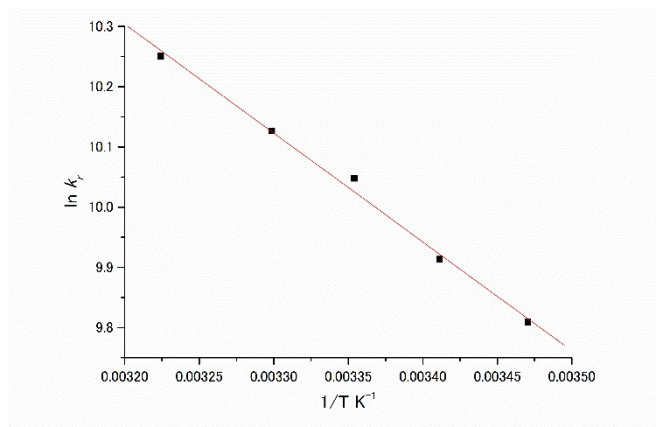


Fig. S16 Arrhenius plot of k_r^D values for reaction (1-D) between α -Toc• and EGCG-D in EtOD/D₂O. The solid line shows the best-fitting line by a standard linear least-squares analysis.

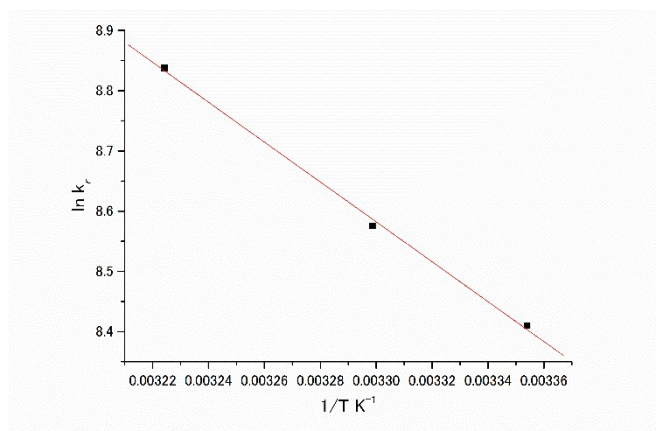


Fig. S17 Arrhenius plot of k_r^H values for reaction (1-H) with MC in EtOH/H₂O. The solid line shows the best-fitting line by a standard linear least-squares analysis.

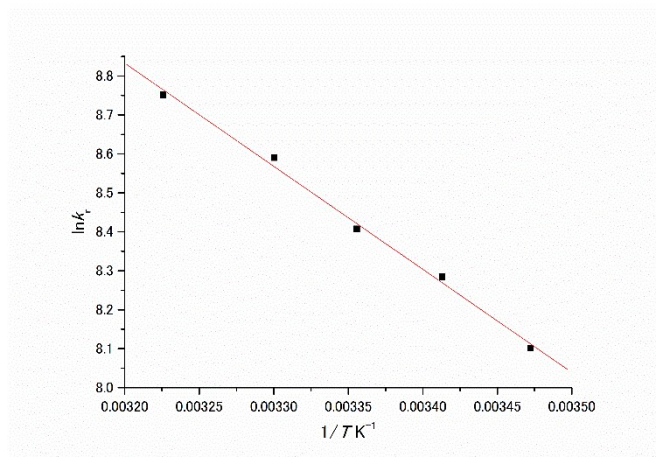


Fig. S18 Arrhenius plot of k_r^H values for reaction (1-H) with MG in EtOH/H₂O. The solid line shows the best-fitting line by a standard linear least-squares analysis.

